## Title

REGGEIZED DOUBLE PERIPHERAL MODEL ANALYSIS OF THREE-BODY FINAL STATE PROCESSES; APPLICATION TO pp -> p n-A++ AT 28.5 GeV/c



## Author

Berger, Edmond L.

## Publication Date

1968-10-18

# University of California

# Ernest O. Lawrence Radiation Laboratory

## REGGEIZED DOUBLE PERIPHERAL MODEL ANALYSIS OF THREE-BODY FINAL STATE PROCESSES; APPLICATION TO $pp \rightarrow p\pi^-\Delta^{++}$ AT 28.5 GeV/c

Edmond L. Berger

October 18, 1968

## DISCLAIMER

Submitted to Physical Review

UCRL-18472
Preprint

UNIVERSITY OF CALIFORNIA

Lawrence Radiation Laboratory
Berkeley, California

AEC Contract No. W-7405-eng-48

# REGGEIZED DOUBLE PERIPHERAL MODEL ANALYSIS OF THREE-BODY FINAL STATE PROCESSES; APPLICATION TO $pp \to p\pi^-\Delta^{++}$ AT 28.5 GeV/c

Edmond L. Berger

October 18, 1968

# REGGEIZED DOUBLE PERIPHERAL MODEL ANALYSIS OF THREE-BODY FINAL STATE PROCESSES; APPLICATION TO $pp \to p\pi^-\Delta^{++}$ at 28.5 GeV/c AND OTHER REACTIONS*

Edmond L. Berger+

Lawrence Radiation Laboratory++
University of California
Berkeley, California

and

Physics Department
Brookhaven National Laboratory
Upton, Long Island, New York

October 18, 1968

## ABSTRACT

Use of a double-Regge-pole-exchange model to describe peripheral three-body final state processes especially at near-threshold values of the invariant mass of a pair of final state particles is described and discussed. Stressed is the fact that the model provides an understanding of the entire reaction, yielding distributions in all kinematical variables. As an example, results are presented from a detailed comparison of the predicted model distributions with data from $pp \to p\pi^-\Delta^{++}$ at 28.5 GeV/c. One simple diagram involving only Pomeranchuk and pion exchanges is employed. Good agreement is obtained with the experimental distributions in invariant-masses, momentum-transfers, and various angles; in particular, the enhancement near 1460 MeV in the $(\pi^-\Delta^{++})$

mass spectrum is well fit. Recent applications of the model to the $A_1$ region in $\pi N \to \pi\rho N$ are reviewed. Also explored is the potential for extracting information on the pion trajectory from three-particle-final-state reaction data.

# I. INTRODUCTION

Extension of the Regge-pole-exchange-model from the quasi-two-body domain to peripheral inelastic processes involving several particles in the final state has been studied by several groups in recent years,[1-4] and phenomenological fits to processes with three particles in the final state have been achieved.[2,4-9] Some of these fits have been carried out within the strict limits of applicability of the Regge-pole model, namely, using only events in that region of the Dalitz plot where the final-state two-particle invariant masses are relatively large. Whereas this limitation can evidently be justified by invoking the origins of Regge theory, it has the unavoidable drawback, at presently accessible energies and current bubble-chamber experiment statistics levels, of leaving one with very few events to study.

On the other hand, recent work with finite-energy sum-rules[10] in two-body scattering demonstrates that the parameterization appropriate to high energy scattering does provide an adequate semi-local average description of low energy phenomena. Thus one is motivated to invoke the same type of result in the multiparticle domain and to suggest that a double-Regge-pole-exchange-model may also, in restricted circumstances, be analytically continued below its designed region of evident validity and provide useful results when one or both two-particle invariant masses become small.[11]

Some results of such an extension have already been described by the author and successful fits to data from several reactions published.[5-7] In this paper, additional characteristic features of the

double-Regge approach are noted and compared with results from non-Reggeized Deck-type models.[12] An important aspect of the double-Regge model approach which deserves emphasis is that it provides an understanding of the entire three-body final state reaction; it yields distributions in all relevant kinematical variables, not merely fits to the Dalitz plot or to one Chew-Low plot.

In Section II, the double-Regge-pole-exchange hypothesis for general three-particle-final-state reactions in the form given by Bali, Chew, and Pignotti[1] is reviewed and, in Section III, the rationale for extending its application to near-threshold values in one of the final state two particle invariant masses is made explicit. These sections are intended to be fairly general and should provide a basis for use of the model in the analysis of an arbitrary three-particle reaction.

A particular example of the use of a double-Regge model at high-energy is focused upon in Section IV. The reaction $pp \to p\pi^-\Delta^{++}$ at 28.5 GeV/c is discussed in some detail and distributions calculated from the double-Regge model are compared with the several experimental distributions.[13] A choice is made of an appropriate unique double-exchange diagram on the basis of certain kinematic selections and then the matrix element is parameterized in terms of two constrained parameters: a scale constant, $s_{0\pi}$, and the slope of the pion trajectory, assumed linear. By adjusting the two parameters, a good fit to the data is obtained; the pion trajectory slope determined in this fashion is $\alpha'_\pi = 1.2(\text{GeV})^{-2}$ and the scale constant $s_{0\pi} = 0.7\ (\text{GeV})^2$, both quite acceptable values and in agreement with the parameters determined

in an earlier modified double-Regge model fit to data on the same reaction at 6.6 GeV/c.[6]

The invariant mass allowed to approach threshold in this calculation is that of the $(\pi^-\Delta^{++})$ system. What emerges is an acceptable fit to the near-threshold 1460 MeV enhancement in this mass spectrum without the necessity of invoking a resonance interpretation of the phenomenon.

In Sections IV. F and V, the more general features of the double-Regge model distributions and particular phenomenological consequences of the model are emphasized and contrasted with results of the non-Reggeized Deck-type models.

The final Section (VI) is devoted to a discussion and interpretation of the results. Included are references to recent work in which the model was applied to the processes $\pi^- p \to \pi^- \rho^0 p$ and coherent $\pi^+ d \to \pi^+ \rho^0 d$ and agreement achieved with the experimentally observed $(\pi\rho)$ mass enhancement in the $A_1$ region.[8,9]

For all reactions studied, a linear pion trajectory with an average slope of approximately 1.0 $(\mathrm{GeV/c})^{-2}$ seems to yield best agreement with the data; the sense in which the pion trajectory slope is determined from this analysis is discussed in Sections IV. B and F.

## II. DOUBLE-REGGE-MODEL

In this section the double-Regge-pole exchange model hypothesis[1-4] is briefly reviewed for the general-mass, three-body-final-state process:

$$m_1 + m_2 \rightarrow \mu_1 + \mu_2 + \mu \quad . \tag{1}$$

Commonly, the assumption of the Regge approach is that the model is strictly applicable only in that central region of the Dalitz-plot where the invariant mass of each final state pair of particles is "large." Whether one uses the Toller variable route[1] or a procedure involving a double Sommerfeld-Watson transformation, this restriction obtains directly because only when the invariant mass is large does the asymptotic expansion yielding an $(s_i)^{\alpha_i}$ type dependence on the sub-energy variable $s_i$ result naturally. The hypothesis asserts that reaction (1) is dominated by a sum of diagrams of the form given in Fig. 1.

Generally stated, in the sum there is a diagram for each possible ordering at the three vertices of the final set of particles relative to the initial pair and, given an ordering, for each unique pair of trajectories whose quantum numbers allow coupling to the external particles. Although this statement means that the analysis for a given process will require many diagrams, limiting consideration to a restricted kinematic region reduces the number of important diagrams. This procedure will be discussed below, after the general situation is pursued here.

For the sake of clarity, in this section all the external particles in the diagram of Fig. 1 will be considered spinless; an helicity-amplitude approach for the general spin case may be found in Ref. 4. For the specific diagram given in Fig. 1, with the mass and trajectory labeling indicated, the invariant amplitude is.[1,2,14,15]

$$A(s,s_1,s_2,t_1,t_2) \approx F_1(t_1)[(s_1\cdots)/s_{10}]^{\alpha_1} F_3(t_1,t_2,\omega)$$

$$\times [(s_2\cdots)/s_{20}]^{\alpha_2} F_2(t_2) \quad . \qquad (2)$$

In this expression, each of the functions $F_i(t_i)$ contain as factors (a) the propagator function for trajectory $\alpha_i(t_i)$, (b) the signature factor for trajectory $\alpha_i$, (c) necessary kinematic factors associated with the coupling of $m_i$ and $\mu_i$ to trajectory $\alpha_i$, and (d) the reduced residue function associated with the $(m_i, \mu_i, \alpha_i)$ coupling. Insofar as they can be determined from Regge fits to quasi-two body processes, these four factors are, in principle, all known quantities.

In Eq. (2), the factors $[(s_i\cdots)/s_{i0}]^{\alpha_i}$ provide the characteristically Regge form of the amplitude; the $s_{i0}$ are scale constants and, judging from two-body fits, $s_{i0} \approx 1\ (\text{GeV})^2$. The quantity $(s_i\cdots)$ is the numerator of the cosh $\xi_i$ variable of Bali, Chew, and Pignotti,[1] the denominator of which is absorbed into $F(t_i)$ and $F(t_1, t_2, \omega)$ as a kinematic singularity. Explicitly, for the general mass configuration of Fig. 1,

$$(s_1 \cdots) = s_1 - t_2 - m_1^2 + \frac{1}{2} t_1^{-1}(\mu_1^2 - m_1^2 - t_1)(\mu^2 - t_1 - t_2) \quad . \tag{3}$$

An analogous expression for $(s_2 \cdots)$ is obtained by interchange of the subscripts 1 and 2 in Eq. (3). The remaining factor in Eq. (2), the function $F(t_1, t_2, \omega)$ describes the coupling of the two Reggeons $\alpha_1$ and $\alpha_2$ at the central vertex to the emitted particle of mass $\mu$. The variable $\omega$, a natural rotation angle in the Toller analysis approach, may be defined as[1,2]

$$\cos \omega = \frac{(\vec{p}_1 \times \vec{q}_1) \cdot (\vec{p}_2 \times \vec{q}_2)}{|\vec{p}_1 \times \vec{q}_1| \; |\vec{p}_2 \times \vec{q}_2|} \quad , \tag{4}$$

where the three-vectors $\vec{q}_i$ and $\vec{p}_i$ are evaluated in the Lorentz frame in which $\vec{q} = 0$, i.e. the rest frame of the particle emerging from the central vertex. As this equation indicates, $\omega$ is the angle between the normals to the $(\vec{p}_1, \vec{q}_1)$ and $(\vec{p}_2, \vec{q}_2)$ production planes, as viewed from the frame of reference in which $\vec{q} = 0$.

The reaction amplitude A on the left-hand-side of Eq. (2) has been expressed as a function of the complete set of independent variables $(s, s_1, s_2, t_1, t_2)$. From the purely kinematic point of view, $\omega$ is not a variable independent of that set; as pointed out most explicitly by Bali, Chew, and Pignotti,[1] $\omega$ is complementary to the total energy variable s. Nevertheless, the range of $\omega$, at fixed s, is not limited: it extends from 0 to $\pi$. Moreover, it is meaningful, even at fixed s, to express the right-hand-side of Eq. (2) in terms of $\omega$

because the two-Reggeon-one-particle vertex function may, in general, have a dynamical dependence on that variable. To be sure, in order to perform an explicit calculation at fixed $s$, the asserted dynamical dependence on $\omega$ must be transformed into a dependence on the chosen set of independent variables. By the same token, because the kinematic relationship between $\omega$ and any one of the set $(s, s_1, s_2, t_1, t_2)$ involves all members of the set, there is no reason to expect the distribution in the variable $\omega$ to be isotropic, even if the function $F(t_1, t_2, \omega)$ should be entirely free of explicit $\omega$ dependence.

The general multi-Regge analysis does not presently specify the dependence of this central-vertex function on $\omega$ and on the $t_i$; barring detailed model calculations, this dependence must be sought-out phenomenologically. This situation is similar to that in the two-body Regge approach in which one determines the $t$ dependence of the reduced residue functions phenomenologically.

For a specific peripheral three particle final state reaction, given the set of relevant doubly-peripheral diagrams [and their amplitudes in the form of Eq. (1)], one presumably has in the double-Regge model a complete description of the physical process. Specifically, one should be able to produce an adequate fit for the distributions in <u>all</u> possible momentum-transfer-, final-state two-particle invariant-mass-, and angular variables. It should be noted that this approach is considerably more ambitious than, for example, the Deck type[12] models which have for the most part been limited to a description of the Chew-Low plot in one momentum transfer and one invariant mass combination for

a given reaction. The process $pp \rightarrow p\pi^{-}\Delta^{++}$ is examined later in this paper as an example of the complete fit stressed above.

The remarks of the previous paragraph are subject, of course, to the qualification that the Regge model is usually considered applicable only when the various two-particle final-state invariant mass values are large. The next section is devoted to a discussion of the reasoning behind extending the Regge model to cover the entire Dalitz plot.

## III. EXTENSION TO SMALL SUBENERGIES

Motivation to apply the double-Regge-pole exchange model below its region of orthodox validity stems from various sources. Empirically, it is interesting to contemplate for a typical process the fraction of data remaining after imposition of the orthodox restriction that all final-state two-particle invariant masses be "large". Take, for example, the reaction $pp \to pn\pi^+$ at incident proton lab momentum 28.5 GeV/c.[13] Barely 4% of the events are left after elimination of those for which either Mass $(n\pi^+) < 2.0$ GeV or Mass $(p\pi^+) < 2.0$ GeV. At current high-energy bubble-chamber experiment statistics levels, therefore, fewer than 50 events would be available for Regge model analysis.[16] Whereas consistency of the model with the data of this limited sample is evidently essential, it is also valuable to attempt to broaden the scope of inquiry.

An analytical understanding of the fact that approximately 96% of the data from $pp \to pn\pi^+$ at 28.5 GeV/c is concentrated in that segment of the Dalitz plot where either Mass $(n\pi^+) < 2.0$ GeV or Mass $(p\pi^+) < 2.0$ GeV is easily given in terms of a doubly-peripheral picture. This issue has been explored quantitatively by various researchers, often in the context of the Deck-effect.[12] An explicit statement in terms of Fig. 1 is this: Although, on purely phase-space grounds, each $s_i$ may range from $(\mu + \mu_i)^2$ to $[(s)^{\frac{1}{2}} - \mu_j]^2$, $j \neq i$, the graph in Fig. 1 implies that both $t_i$ are heavily weighted towards their maximum (kinematic) limiting values (e.g. $t_i$ weighted near 0 if $\mu_i > m_i$) which, in turn, substantially kinematically

distorts the phase-space spectrum in the $s_i$. Indeed the restriction of either $t_i$ to values near its absolute kinematic limit has the effect of enhancing small values of both $s_i$. Consequently there is an incompatibility between the assertion of double-peripherality on the one hand and the orthodox requirement of a multi-Regge model which would have the masses of all pairs of final state particles large.

Relaxation of the restriction to large $s_i$ finds support in the many recent successful applications of finite-energy-sum-rules, in two-body reactions, in which the low-energy direct-channel resonance approximation has provided a good description of various cross-channel Regge trajectories.[10] The import of this development for three-particle reactions has been emphasized by Chew and Pignotti.[11] What emerges is the suggestion that in using the double-Regge model one should expect to achieve a reasonably good semi-local-average description of the data over the complete spectrum of $s_i$ values. Certainty sharp resonance-like detail cannot result, but gross features of the $s_i$ and other distributions should be well reproduced. Particularly interesting, therefore, from the point of view of phenomenological application of the model, are investigations of those particular three-body reactions which either display essentially no resonant effects in any subenergy[17] variable, or display fairly structureless, broad enhancements at low invariant mass values of one pair of final state particles. Several examples of this latter type will be discussed later in this paper.

Finally, the multi-Regge theory approach to several-particle-production[1] would be facilitated by a convincing demonstration in the

three-particle arena that the use of a double-Regge approach at small subenergies is in acceptable agreement with experiment, especially in the sense of generating a suitable average over the resonance-region. The demonstration would help to justify a multi-Regge description of multiple production which ignores resonances and concentrates rather on computing with diagrams having only stable particles in the final state.

In order to restrict the number of diagrams treated, the approach taken here was to relax the orthodox Regge-theory limitation in the case of one subenergy variable only. An example of a calculation of this type is given in the next section.

## IV. APPLICATION TO $pp \to p\pi^-\Delta^{++}$

A double-Regge model analysis for the reaction $pp \to p\pi^-\Delta^{++}$ is described in this section in a manner general enough to allow similar application, for example, to $pp \to \pi pp$, $\pi p \to \pi\pi p$, $\pi p \to \pi\rho p$, $Kp \to \pi K\Delta$, $Kp \to \pi K^* p$, and analogous coherent processes. Predictions of the Regge model are compared here with experimental distributions obtained by a Brookhaven group studying proton-proton interactions at 28.5 GeV/c.[13]

### A. Choice of Diagrams

The essential simplifying conclusion reached in this section is that by limiting the study to events for which Mass $(p\pi^-) > 2.0$ GeV, one may adequately represent the data with a unique double-exchange diagram, given in Fig. 3(a), employing Pomeranchuk and pion exchanges only. Other possible diagrams are judged to provide contributions of secondary importance.

Since the incident particles in $pp \to p\pi^-\Delta^{++}$ are identical, there are a priori only three generic types of double-Regge-pole-model diagrams which can be written for this process, differing according to which final-state particle is coupled at the central two-Reggeon-one-particle-vertex. The quantum number structure of two of these types, with either $\pi$ or $\Delta$ emerging from the central vertex, is such that a Pomeranchuk (P) can be accommodated as one of the pair of exchanged Reggeons. The third type of diagram, with a proton emitted at the middle vertex, cannot admit P exchange.

Separate consideration of diagrams with and without P exchange is justified by various arguments. One line of argument is

based on the fact that for a diagram containing P exchange the total cross section, $\sigma$, is approximately s independent whereas $\sigma$ falls with s if P exchange is not present. Another line of reasoning relates to the fashions in which various exchanges populate the allowed ranges of the various subenergies. Because of the characteristic $(s_i/s_0)^{\alpha_i}$ subenergy dependence in the amplitude, the contribution of the Pomeranchuk trajectory $(\alpha_P \approx 1)$ will dominate when the associated subenergy is large. In fact, the P will most effectively overcome the preference, discussed earlier, of double-peripheral diagrams for small subenergies. On the other hand, the lower lying a given trajectory, the closer to threshold in the associated subenergy will its contribution be felt.

In regard to the specific process under study here, the restriction to events with Mass $(p\pi^-) > 2.0$ GeV should be sufficient to justify the disregard in first approximation of all diagrams other than those containing P exchange. The two diagrams of interest remaining are drawn in Fig. 2, where the meson (M) and baryon (B) exchanges must now be specified.

Quantum number requisites at the central vertex of Fig. 2(a) demand that M have G parity (-1) and isospin 1; the obvious candidates are $\pi$ and $A_1$. The standard nearest singularity argument suggests that the $\pi$ contribution is dominant over that of $A_1$ at small values of the momentum transfer to the $\Delta^{++}$. In addition, a comparison of the on-mass-shell $\pi p$ elastic and $\pi p \to Ap$ cross-

sections shows that the strength of the $\pi\pi P$ coupling is a factor of 10 greater than the $\pi$-A-P coupling; because such coupling constants enter at the middle vertex of the two diagrams, $\pi$ exchange would appear to be substantially favored. For Fig. 2(b), the argument is similar with the conclusion being that the baryon B is the $\Delta^{++}$ itself.

The diagrams of Fig. 2 contribute to overlapping regions of phase space, and a meaningful separation of their contributions requires limitations on $t_\Delta$ and $t_\pi$. Kinematically, although the maximum value of $t_\pi$ is given by $(m_p - m_\pi)^2 \approx +0.6\ (\mathrm{GeV})^2$, a distance-from-the-baryon-pole discussion can be used to argue that the magnitude of the contribution of Fig. 2(b) should be suppressed in relation to that of Fig. 2(a); interference questions are more delicate. The easily derived relationship

$$t_\pi + t_\Delta = t_p - s_{\pi\Delta} + m_p^2 + m_\Delta^2 + m_\pi^2 \quad , \tag{5}$$

indicates, however, that interference is important only in regions of phase space distant from both poles, for example, where $t_\Delta < -0.5\ (\mathrm{GeV})^2$.

Finally, to facilitate comparison with the limited quantity of data, only the pion-Pomeranchuk diagram given in Fig. 3(a) was retained in the detailed computations. Because of the approximations discussed thus far, certain qualifications as to the expected results are evident. One should not expect to compute with this one diagram the entire observed cross section. Moreover, in adjusting free parameters associated with Fig. 3(a) in an attempt to fit data, one will perforce be generating some type of average over the background associated with neglected diagrams.

## B. Matrix Element

The invariant amplitude for the diagram in Fig. 3(a) will be written as a function of the set of five Lorentz-invariant quantities defined in terms of the four momenta $p_i$ and $q_i$ as $s = (p_1 + p_2)^2$, $t_\Delta = (q_2 - p_2)^2$, $t_p = (q_1 - p_1)^2$, $s_{\pi\Delta} = (q + q_2)^2$, and $s_{p\pi} = (q + q_1)^2$. The differential cross section for the process is

$$d\sigma = (2\pi)^{-5} (4F_I)^{-1} (\sum|M|^2)\, d\varphi_3 \ , \qquad (6)$$

in which $F_I$ equals the proton mass times the incident proton lab momentum, and $d\varphi_3$ is the differential element of phase space.

The complexities of spin analysis were set aside by the adoption of the double-Regge-pole hypothesis for the absolute square of the invariant amplitude, M, summed over final spins and averaged over initial spins.[1,2] This effective neglect of spin dependence has the practical consequence of reducing the number of parameters involved in describing the momentum transfer ($t_p$ and $t_\Delta$) structure of the amplitude. In the paragraphs below, a description is given of the fashion in which this spin-averaged momentum transfer dependence was specified. The explicit dependence of the amplitude on the subenergy variables (and thus on the trajectories) is not affected by the averaging, however, since each helicity amplitude[4] contains a common factor $(s_{\pi p}\cdots)^{\alpha_P}(s_{\pi\Delta}\cdots)^{\alpha_\pi}$ which can be extracted to provide the overall dependence on the subenergies.

The discussion of the parameterization of $\sum|M|^2$ is based upon the functions $F_i$ of Eq. (2). Because the model yields no

prescription for the $\omega$ dependence of $F_3(t_\Delta, t_p, \omega)$, such explicit variation was initially assumed absent here. This assumption seems justified by the resulting fits, especially by the fit to the distribution in $\omega$ itself, shown in Fig. 6(b).

In the attempt to reduce the number of free parameters, information obtainable from quasi-two-body reaction studies was incorporated into the specification of the $t_\Delta$ and $t_p$ dependences of $(\sum |M|^2)$. Because fits[18] to two-body data conclude that the Pomeranchuk has little slope, if any, the P was chosen here to be a fixed singularity, $\alpha_P = 1.0$. Thus there is no P propagator to be discussed. For definiteness, the scale constant $s_{0P}$ was set equal to 1.0 $(GeV)^2$, and then the remaining $t_p$ dependence of the amplitude [in the product $F_1(t_p)\, F_3(t_p, t_\Delta)$ of Eq. (2)] was parameterized as an exponential function determined from high-energy $\pi p$ elastic scattering data, as follows: In the limit $t_\Delta \to m_\pi^2$, $t_p$ is simply the invariant momentum transfer variable for $\pi p$ elastic scattering and the function $F_3(t_p, t_\Delta)$ becomes an external residue; thus, in that limit, the product $F_1(t_p)\, F_3(t_p, t_\Delta)$ is proportional to t dependence the amplitude for the elastic $\pi p$ process. Under the assumptions (1) that for small $t_\Delta$, the $t_p$ dependence of the product $F_1(t_p)\, F_3(t_p, t_\Delta)$ differs little from the on-shell case and (2) that the Pomeranchuk is responsible for the $\pi p$ elastic diffraction peak,[19] it is appropriate to set $|F_1(t_p)\, F_3(t_p, t_\Delta)|^2 \approx F_3'(t_\Delta) \exp(8t_p)$ where $F_3'(t_\Delta)$ is an unknown slowly varying function.

The discussion of the previous paragraphs may be summarized in the following expression for the amplitude[20] corresponding to the

diagram of Fig. 3(a):

$$\sum |M|^2 = N_0 \, G_\pi(t_\Delta)[(s_{\pi\Delta}\cdots)/s_{0\pi}]^{2\alpha_\pi}(s_{\pi p}\cdots)^2 \exp(8t_p) \quad . \qquad (7)$$

Details of the $\pi$ coupling to $p\Delta$ as well as the $\pi$ propagator and the residual middle vertex $t_\Delta$ dependence, previously denoted $F_3'(t_\Delta)$, are incorporated into $G_\pi(t_\Delta)$, and $N_0$ is the overall normalization constant.

$$(s_{\pi\Delta}\cdots) = s_{\pi\Delta} - t_p - m_p^2 + \frac{1}{2} t_\Delta^{-1}(m_\Delta^2 - m_p^2 - t_\Delta)$$

$$\times (m_\pi^2 - t_p - t_\Delta) \quad . \qquad (8)$$

$$(s_{\pi p}\cdots) = s_{\pi p} - t_\Delta - m_p^2 - \frac{1}{2}(m_\pi^2 - t_p - t_\Delta) \quad . \qquad (9)$$

The characteristics of the pion trajectory are, at present, an issue of intense investigation in two particle scattering and, as such, it is hardly possible to present a well-established expression for $G_\pi(t_\Delta)$. In this study the most natural assumptions consistent with Regge theory phenomenology were made. A linear pion trajectory was adopted,

$$\alpha_\pi = (t_\Delta - m_\pi^2) \cdot \alpha_\pi' \quad , \qquad (10)$$

with the constant slope, $\alpha_\pi'$, left as an adjustable parameter; $G_\pi(t_\Delta)$ was assumed to be given entirely by the product of the Reggeized propagator and signature factor with no other vertex structure:

$$G_\pi(t_\Delta) = \frac{(\pi\,\alpha'_\pi)^2}{2(1 - \cos \pi\,\alpha_\pi)} \quad . \tag{11}$$

It will be noted that for $t_\Delta \to m_\pi^2$, $G_\pi(t_\Delta)$ approaches the elementary OPE expression: $G_\pi(t_\Delta) \to (t_\Delta - m_\pi^2)^{-2}$.

The expression for $G_\pi(t_\Delta)$ in Eq. (11) is not appropriate for large values of $|t_\Delta|$ [i.e. $|t_\Delta| > 1.0\ (\mathrm{GeV}/c)^2$] because, as it stands, it develops poles in the physical region at $\alpha_\pi = -2, -4$, etc. These unphysical poles could be eliminated by restoring to the right-hand-side of Eq. (11) the factor $[\Gamma(1 + \alpha)]^{-2}$ sometimes used in Regge-pole phenomenological fits.[21] However, because pion exchange is dominant only for small $t_\Delta$, a cutoff in the integration over the $t_\Delta$ variable (and in the data) is appropriate here for physical reasons, and the difficulty is thus avoided.

Two adjustable parameters which may be varied to achieve a fit to the shapes of the several experimental distributions are embodied in Eqs. (7) and (10). They are both associated with the pion exchange aspect of the diagram and are the slope, $\alpha'_\pi$, of the pion trajectory function and the scale constant $s_{0\pi}$.

In one-Regge-pole-exchange fits to quasi two body reaction data over a range of $s$ values, it is possible to isolate the trajectory function $\alpha(t)$ from the remaining $t$ dependence of the amplitude by fitting the differential-cross-section, at fixed $t$ for various $s$, to an expression of the form

$$\frac{d\sigma}{dt} = f(t)\left(\frac{s}{s_0}\right)^{2\alpha(t)-2} \quad . \tag{12.a}$$

Technically, a similar program could be undertaken in this three-body reaction to separate the $\alpha'_\pi$ and $s_{0\pi}$ dependences of the amplitude; its results are inconclusive because of the limited quantity of data, however. The procedure requires performing the integrations over the $(s_{\pi p}\cdots)$ and $t_p$ variables in Eq. (6) and (7) to obtain a doubly-differential cross section in the $s_{\pi\Delta}$ and $t_\Delta$ variables:

$$\frac{d^2\sigma}{dt_p\, d(s_{\pi\Delta}\cdots)} = G_\pi(t_\Delta)\,[(s_{\pi\Delta}\cdots)/s_{0\pi}]^{2\alpha_\pi}\, K[s,\, t_\Delta,\, (s_{\pi\Delta}\cdots)] \quad . \tag{12.b}$$

The function $K$ in Eq. (12.b) will be a known quantity. If one then substitutes empirical data, at a fixed $t_\Delta$, for the left-hand side of Eq. (12.b), the $(s_{\pi\Delta}\cdots)$ dependence of the ratio $K^{-1}\, d^2\sigma/dt_\Delta\, d(s_{\pi\Delta}\cdots)$ will provide a value for $\alpha_\pi(t_\Delta)$, at that $t_\Delta$, which is independent of $s_{0\pi}$ and, moreover, of the parameterization of $G_\pi(t_\Delta)$. As remarked, the limited statistics precluded using this procedure except as a consistency check.

In view of the fact that one may express $(s_{0\pi})^{-2\alpha_\pi}$ as $\exp[-2(t_\Delta - m_\pi^2)\,\alpha'_\pi \log s_{0\pi}]$, it is evident that changing $s_{0\pi}$ will serve to modify an inherent exponential damping in the variable $t_\Delta$. Varying $\alpha'_\pi$ will directly affect the shapes of distributions in both $s_{\pi\Delta}$ and $t_\Delta$. It is to be expected therefore, that for a limited

statistics sample of data, various pairs of the quantities $\alpha'_\pi$ and $s_{0\pi}$ will generate successful fits. As will be stressed later, however, the data do require that $\alpha'_\pi \approx 1.0\ (\mathrm{GeV/c})^{-2}$; an elementary pion-exchange calculation fails in a well-defined manner, which supports the argument given here that the amplitude representing the data must contain a factor like $(s_{\pi\Delta})^{\alpha_\pi}$ with $\alpha_\pi < 0$. These issues are discussed further in subsection IV.F.

## C. Normalization

The normalization factor $N_0$ of Eq. (7) was determined by factoring the diagram of Fig. 3(a) about the pion exchange line and considering the limit $t_\Delta \to m_\pi^2$. The contribution to $N_0$ of the $p\Delta\pi$ vertex, in that limit, may be evaluated in terms of the width, $\Gamma$, and mass $m_\Delta$ of the $\Delta^{++}$ as the factor[22]

$$g_\Delta^2 = 32\pi\, \Gamma\, m_\Delta^3 \{[m_\Delta + m_p)^2 - m_\pi^2][(m_\Delta - m_p)^2 - m_\pi^2]\}^{-\frac{1}{2}} \quad . \tag{13}$$

The remainder of the diagram represents off-mass-shell $\pi p$ elastic diffraction scattering as may be recognized if Eq. (7) is rewritten as

$$\sum |M|^2 = g_\Delta^2\, G_\pi(t_\Delta) \left( \frac{s_{\pi\Delta} \cdots}{s_{0\pi}} \right)^{2\alpha_\pi} \left( \sum |M'_{\pi p}|^2 \right) \quad , \tag{14}$$

where $M'_{\pi p}$ is the amplitude for off-shell $\pi p$ elastic diffraction scattering. In the diffraction peak approximation,[19]

$$\sum |M'_{\pi p}|^2 \approx \left( \sum |M'_{\pi p}|^2 \right)\Big|_{t_p=0} \exp(8t_p) \quad . \tag{15}$$

Moreover by using the optical theorem and assuming a purely imaginary amplitude at $t_p = 0$, as is the case for P exchange, one may derive the expression[23]

$$\sum|M'_{\pi p}|^2 \approx [s_{p\pi} - (m_p + m_\pi)^2][s_{p\pi} - (m_p - m_\pi)^2]$$

$$\times \sigma_{tot,\pi p}^2 \exp(8t_\Delta) \quad , \qquad (16)$$

where $\sigma_{tot,\pi p}$ is the $\pi p$ total cross section. After combining Eqs. (14) and (16), and comparing the result with Eq. (7) (at large $s_{p\pi}$ and small $t_p$ and $t_\Delta$), one obtains[24]

$$N_0 = 2 g_\Delta^2 \sigma_{tot,\pi p}^2 \quad . \qquad (17)$$

A factor of 2 was inserted into Eq. (17) because antisymmetrization of the reaction amplitude is required since the incident particles are identical. This effect is properly obtained by adding to Fig. 3(a) a diagram in which the incident particle momenta are interchanged. Due to the peripheral nature of the process, however, interference between the two diagrams is entirely negligible.

## D. Data

A few remarks concerning the experimental distributions are in order before actual fits are described. When the mass spectrum of the final $(p\pi^+)$ combination in data from the four-prong reaction $pp \to pp\pi^+\pi^-$ is plotted, a strong $\Delta^{++}$ signal is evident. However, if one selects just those events from the broad enhancement $M(p\pi^+\pi^-) < 1600$ MeV, and then displays the $(p\pi^+)$ mass spectrum, it is less clear that a prominent $\Delta^{++}$ component is present, partially

due to limited statistics and partially due to the fact that the three-body mass selection already kinematically constrains the two-particle mass to overlap the $\Delta^{++}$ band. This ambiguity is disturbing because there are at least two theoretical exchange mechanisms, alternative to $p\pi^-\Delta^{++}$, which may also serve to generate a broad low-mass $(p\pi^+\pi^-)$ enhancement. One involves the assumption that the process is actually $pp \rightarrow pp\sigma$ where $\sigma$ is an s wave two-pion resonance.[25] Another is based on the fact that the yield of a triple-exchange process such as diagrammed in Fig. 3(b) will be largely in the region of small $(p\pi^+\pi^-)$ mass values. In an attempt to overcome both of these objections, the assertion made here is that if a relatively narrow $\Delta^{++}$ mass definition is used [Mass$(p\pi^+)$ = 1238 ± 60], one will be left with data in which the true $\Delta^{++}$ to background signal is high. Note that the cut discussed earlier, Mass$(p\pi^-) > 2.0$ GeV, will remove double isobar events of the $N^{*0}\Delta^{++}$ variety.

The data on the final state $p\pi^-\Delta^{++}$ thus derived from $pp \rightarrow pp\pi^+\pi^-$ is produced highly peripherally with small momentum transfers to the $\Delta^{++}$ and to the p. The experimenters have noted, however, that there is a biased loss from the present sample of those events having $|t_p|$ very small and associated with the $(\Delta^{++}\pi^-)$ being in the forward hemisphere.[13] This loss is serious primarily for $|t_p| < 0.04$ $(\text{GeV}/c)^2$, and consequently, rather than limiting the study to the smaller statistics unbiased $(\Delta^{++}\pi^-)$- backwards sample, all events were retained.

## E. Fit to Data

Attention was focused principally on the limited high-statistics region defined by $\{s_{p\pi} \geq 4.0,\ s_{\pi\Delta} \leq 5.0,\ |t_{\Delta}| \leq 0.5,\ |t_{p}| \leq 0.5,$ all units $(\text{GeV})^2\}$, where effects from diagrams other than the dominant one are expected to be negligible. Various pairs of the parameters $\alpha'_{\pi}$ and $s_{0\pi}$ in Eq. (7) provide acceptable fits in the sense of generating sets of singly differential distributions whose shapes agree with those of corresponding experimental distributions. A maximum likelihood fit to the data, in the four-dimensional space of the two subenergy and two momentum transfer variables, produced the values $\alpha'_{\pi} = 0.8 \pm 0.2\ (\text{GeV})^{-2}$ and $s_{0\pi} = 0.50 \pm 0.05\ (\text{GeV})^2$; however, the limited number of events involved and the biases discussed earlier reduce confidence in this determination.[26] As judged by eye, a somewhat better fit to the shapes of the several distributions results from the choice of $\alpha'_{\pi} = 1.2\ (\text{GeV})^{-2}$ and $s_{0\pi} = 0.7\ (\text{GeV})^2$. Presented in Figs. 4 through 7 are singly differential distributions computed using the latter pair of values. Naturally the same selections were made in the computation as taken in the data; these are described in the captions. Good fits resulted also to the doubly-differential distribution $d^2\sigma/dt_{\Delta}\, ds_{\pi\Delta}$ and, as well, to that in the variable $t_{\pi} = (q - p_2)^2$, which should be sensitive to the neglected baryon-exchange-diagram's contribution. The values determined for the pair of quantities $\alpha'_{\pi}$ and $s_{0\pi}$ are well in line with the typical slopes and scale parameters of Regge theory and, moreover are in close

agreement with values obtained for the same parameters in a fit to data at the much lower momentum of 6.6 GeV/c.[6]

Because the constant term, $N_0$, in Eq. (7) cancels out in the definition of the likelihood function, the maximum likelihood fit is to the shape of the distribution of events in the $(s_{\pi\Delta}, s_{p\pi}, t_\Delta, t_p)$ space only and not to the absolute normalization. Similarly, the fits carried out by eye were to shapes only. Thus the degree of agreement between model and data in terms of absolute normalization is a measure of the extent to which the diagram of Fig. 3(a) indeed dominates the reaction. The actual Regge-model curves shown in Figs. 4 through 7 were obtained after multiplying Eq. (7) by the factor 0.95, while the other pair of values $[\alpha'_\pi = 0.8\ (\text{GeV})^{-2}$ and $s_{0\pi} = 0.5\ (\text{GeV})^2]$ yield a cross section which is 96% of the experimental value.[27] Consequently, the absolute normalization aspect of the model is remarkably good, as it was also at 6.6 GeV/c.[6]

## F. Discussion of the Fit

It is evidently not possible to prove in a rigorous sense that this data (or any data in the physical region, $t_\Delta < 0$) demands the existence of the pole singularity postulated here in $G_\pi(t_\Delta)$, Eq. (11), at the unphysical point $t_\Delta = m_\pi^2$. However, the good agreement in absolute normalization ahd the reasonableness of the values determined for $\alpha'_\pi$ and $s_{0\pi}$ demonstrate strong consistency of the pion-exchange aspect of the model with the experimental situation.

On the other hand, it is important to inquire into the role played by Reggeization in this problem.

The finite, positive value for the slope, $\alpha'_\pi$, of the trajectory of the exchange pion, operating through the factor $(s_{\pi\Delta})^{2\alpha_\pi}$ in Eq. (7), is indeed essential in order to generate a distribution in the $(\pi^-\Delta^{++})$ invariant mass whose peak position and full-width at half maximum are in agreement with the data, and in order to produce the type of asymmetry observed in the distribution in the Treiman-Yang angle, Fig. 6(a). These two features of the Reggeized approach may be recognized most directly by contrasting the form and results of this model with those of an elementary one-pion-exchange-diffraction-scattering (OPE-DS) or Deck model[12] which the Reggeized model essentially becomes in the limit $\alpha'_\pi \to 0$.

In the OPE-DS model, one replaces Eq. (7) by[12,28]

$$\sum |M|^2_{OPE} = N_0(t_\Delta - m_\pi^2)^{-2}[s_{p\pi} - (m_p + m_\pi)^2][s_{p\pi} - (m_p - m_\pi)^2] \times$$

$$\times \exp[8t_p + \lambda\cdot(t_\Delta - m_\pi^2)] \quad . \qquad (18)$$

In Eq. (18), $N_0$ has the same value given previously in Eq. (17), and the option of a form factor $\exp[\lambda(t_\Delta - m_\pi^2)]$ has been explicitly introduced (without it the experimental distribution in $t_\Delta$ cannot be fit). At small values of $|t_\Delta|$, the essential difference between Eq. (18) and Eq. (7) is the presence in Eq. (7) of the factor $(s_{\pi\Delta}\cdots)^{2\alpha_\pi}$.

At the energy being considered here, Eq. (18) will yield the same curve for the distribution in $t_\Delta$ as that given by the Regge model, shown in Fig. 4(a), if in Eq. (18), $\lambda \equiv 1.0\ (\text{GeV})^{-2}$. With $\lambda$ therefore fixed at $1.0\ (\text{GeV})^{-2}$, Eq. (18) was used to compute the expected OPE-DS distribution in the $\pi^-\Delta^{++}$ invariant mass. The results of the two models are compared in Table I. Whereas the Regge model is able to adequately fit the distributions in both $t_\Delta$ and $s_{\pi\Delta}$, the OPE-DS model (even with form-factor) can reproduce only one of the two.

Phase-space threshold effects, of course, compel the distribution in $s_{\pi\Delta}$ to vanish at threshold and, as discussed elsewhere, the peaking of the cross section at near-threshold values of $s_{\pi\Delta}$ is largely a kinematic reflection of the suppression of large values of $t_\Delta$ and $t_p$ in the doubly-peripheral diagram. However, Reggeization enhances the low-mass peaking by directly providing an $s_{\pi\Delta}$ dependent factor in the matrix element whose effect is to further suppress large values of $s_{\pi\Delta}$. Analytically, this narrowing of the low-mass enhancement can be understood by observing that the $(s_{\pi\Delta})^{2\alpha_\pi}$ term in Eq. (7) is roughly approximate to $(s_{\pi\Delta})^{-0.3}$ because $\alpha_\pi = (t_\Delta - m_\pi^2)\cdot\alpha'_\pi$ and the peak in the $t_\Delta$ distribution occurs at $t_\Delta \approx -0.12\ (\text{GeV/c})^2$ [see Fig. 4(a)].

In the last row of Table I and in Fig. 6(a), the predictions of the two models for the distribution in the Treiman-Yang angle $\varphi$ are contrasted. The OPE-DS model produces a perfectly flat distribution in the variable $\varphi$ whereas the Regge model yields an asymmetry

about 90° and a peaking toward 0° similar to that observed in the data. In this work, the computed asymmetry about 90° is defined by

$$A = \frac{\frac{d\sigma}{d\varphi}(0°) - \frac{d\sigma}{d\varphi}(180°)}{\frac{d\sigma}{d\varphi}(0°) + \frac{d\sigma}{d\varphi}(180°)} \quad . \tag{19}$$

The physical reason for the large asymmetry developed by the Regge model rests simply, again, in the factor $(s_{\pi\Delta})^{2\alpha_\pi(t_\Delta)}$; this coupling of the adjacent momentum transfer, $t_\Delta$, and subenergy, $s_{\pi\Delta}$, variables may be reexpressed in terms of momentum variables and implies a correlation of the momenta of the particles in the final state. Stated otherwise, the sets $(s, s_{p\pi}, t_\Delta, t_p, s_{\pi\Delta})$ and $(s, s_{p\pi}, t_\Delta, t_p, \varphi)$ are two complementary sets of independent variables in terms of which the amplitude may be expressed. They are related through an expression of the form

$$s_{\pi\Delta} = A(t_\Delta, t_p, s_{p\pi}) + \cos\varphi\, B(t_\Delta, t_p, s_{p\pi}) \quad , \tag{20}$$

which shows that a dependence in the amplitude on $s_{\pi\Delta}$ leads in general to a nonisotopic $\varphi$ distribution. Absence of $s_{\pi\Delta}$ or $\varphi$ dependence in $(\sum |M|^2)$ automatically leads to a perfectly flat distribution in the $\varphi$ variable.

The asymmetry about 90° in the $\varphi$ distribution, quite sensitive to the value of $\alpha'_\pi$, increases as $\alpha'_\pi$ increases. Moreover, for fixed $\alpha'_\pi$, it is also an increasing function of the variable $|t_\Delta|$ because $|\alpha_\pi|$ increases with $|t_\Delta|$; for example, if instead of restricting the

$t_\Delta$ integration to values $|t_\Delta| \leq 0.8$ (GeV/c)$^2$, as in Fig. 6(a) and Table I, one chooses the cut $|t_\Delta| \leq 0.3$ (GeV/c)$^2$, the predicted asymmetry is reduced to 28%. On the other hand, a fixed constant power behavior in the variable $s_{\pi\Delta}$ would lead to an asymmetry which is independent of $t_\Delta$. The data at both 6.6 GeV/c[6,29] and 28.5 GeV/c give definite evidence for an increase in the asymmetry as one takes progressively larger cuts in $|t_\Delta|$ and are thus highly suggestive of a mechanism whereby the spin of the exchanged object is a function of $t_\Delta$.

The validity of the conclusions presented in the above paragraphs does not rely upon the very simple form chosen for the $t_\Delta$ dependence of $(\sum |M|^2)$, namely, the function $G_\pi(t_\Delta)$ in Eq. (11). Other more complicated expressions (for example, $G_\pi(t_\Delta)$ multiplied by $[\Gamma(1+\alpha)]^{-2}$) were tried with the result that although $s_{0\pi}$ is forced to change, acceptable fits to the $s_{\pi\Delta}$ and $\varphi$ distributions definitely require that $\alpha'_\pi \approx 1.0$ (GeV/c)$^{-2}$. The criticism may be leveled, of course, that one is misapplying the pion exchange concept when using it as far out in $t_\Delta$ as $|t_\Delta| \approx 0.5$ (GeV/c)$^2$. However, even when one restricts the analysis to $|t_\Delta| < 0.2$ (GeV/c)$^2$ = 10 $m_\pi^2$, the experimental anisotropy in the $\varphi$ distribution is evident and requires $\alpha'_\pi \approx 1.0$ for its interpretation within the context of this model. It would be valuable to pursue this matter of the pion trajectory parameters by analyzing high statistics data on the several reactions listed at the beginning of Section IV.

In the remainder of this section, additional comments are made regarding the distributions presented in Figs. 4 through 7. The discrepancy between the Regge fit and the data for values of $|t_p| < 0.04$ $(GeV/c)^2$, shown in Fig. 4(b) is attributable to the bias, discussed earlier, which results in a loss of events at small $|t_p|$ when the $(\Delta^{++}\pi^-)$ system is in the forward hemisphere. Indeed, the dashed histogram in the region $|t_p| < 0.04$ $(GeV/c)^2$ corresponds to twice the number of events present in the backwards $(\Delta^{++}\pi^-)$ sample; this bias is not serious in the remainder of the $|t_p|$ distribution. Because events with $|t_p| < 0.04$ $(GeV\Delta c)^2$ occur preferentially with small values of $s_{\pi\Delta}$, this bias explains, in part, the apparent normalization discrepancy in the distribution in the $s_{\pi\Delta}$ variable, Fig. 5(a). The effects of the bias on the other distributions is negligible. The distribution in the $s_{p\pi}$ variable, Fig. 6(b) shows that the $(s_{p\pi}\cdots)^2$ factor in Eq. (7), characteristic of Pomeranchuk exchange or diffraction scattering, is a good representation of the overall $s_{p\pi}$ dependence for values $s_{p\pi} \geq 4.0$ $(GeV)^2$, as asserted earlier. The agreement at the lower end of the scale can be improved by the addition of a diagram with P' exchange, for example; moreover a mild slope[18] $(\alpha'_p \simeq 0.3)$ for the Pomeranchuk results in better agreement of the shape of the calculated distribution with the data at the upper end of the spectrum. The agreement evident in Fig. 6(b) suggests that the choice made here to ignore explicit $\omega$ dependence in the two-Reggeon-one-particle vertex is quite consistent with the experimental situation.

The severe cuts $|t_p| < 0.3\ (\mathrm{GeV/c})^2$ and $\mathrm{Mass}(\pi\Delta) < 1.6$ GeV in Fig. 7 were chosen in order to focus on the region of the low mass $(\pi\Delta)$ enhancement. The additional cut, $s_{p\pi} \geq 4.0\ (\mathrm{GeV})^2$, necessary in order to eliminate double-isobar events, removes events in the region $\cos\theta_\Delta > 0.5$. The data show evidence for a depletion of events for $\cos\theta_\Delta < -0.5$; these events are statistically associated with values $|t_\Delta| > 0.5\ (\mathrm{GeV/c})^2$. The discrepancy between the calculated curve and the data for $\cos\theta_\Delta < -0.5$ is perhaps indicative of interference between the principal diagram, Fig. 3(a), and others (such as the $\Delta^{++}$ exchange possibility discussed earlier) in the region $|t_\Delta| > 0.5\ (\mathrm{GeV/c})^2$. Both the calculated curve and the data become peaked towards $\cos\theta_\Delta = +1$ for larger values of $\mathrm{Mass}(\pi\Delta)$.

## G. Conclusions

The overall fit to the data supports the double-Regge-pole exchange approach to three particle production and, in particular, calls for the exchange of a Reggeized pion whose average slope in the momentum transfer range $0 > t > -0.5\ (\mathrm{GeV/c})^2$ is approximately $1.0\ (\mathrm{GeV})^{-2}$. Diagrams other than the dominant one shown in Fig. 3(a) provide negligible contributions to the process $pp \to p\pi^-\Delta^{++}$, at least in the limited domain defined at the beginning of Section IV.E. The low-mass $(\pi^-\Delta^{++})$ enhancement and related distributions are adequately fit without requiring any explicit $(p\pi^+\pi^-)$ resonance production. The neglect of spin effects in the spin-average approach taken here, expecially as regards the $\Delta^{++}$, would not appear to alter these conclusions in view of the fact that the coupling of the pion to the 3/2 helicity states of the $\Delta$ is known from quasi-two body final state data to be a small effect.[30]

## V. FEATURES OF THE MODEL

The discussion in Section IV.F regarding the $s_{\pi\Delta}$ and $\varphi$ distributions underscored some general aspects of the Regge model matrix element and fits. In this section, a few additional features will be stressed.

### A. Slopes in the Momentum Transfer Variable

A particularly interesting consequence of the doubly-peripheral approach becomes evident when one examines the distribution in the variable $t_p$ for various choices of the invariant mass, $M_{\pi\Delta}$, of the $(\pi^-\Delta^{++})$ combination. In a missing-mass type of counter experiment, these are essentially the two relevant variables when one triggers on a fast proton;[31] they are also, of course, the usual variables in a Chew-Low plot. The calculated doubly-differential distribution $d^2\sigma/dt_p dM_{\pi\Delta}$ is in fact well approximated in the region $|t_p| < 0.3\ (\mathrm{GeV}/c)^2$ by the expression

$$\frac{d^2\sigma}{dt_p\ dM_{\pi\Delta}} \approx \exp(a + bt_p) \quad , \tag{21}$$

where the parameters $a$ and $b$, although independent of $t_p$, depend strongly on $M_{\pi\Delta}$. In Table II, values of $b$, for various $M_{\pi\Delta}$, are presented. Also given in the table are the calculated values of $b$ vs. Mass $(n\pi^+)$ for the recently published study of $pp \to pn\pi^+$ at 28.5 GeV/c.[7]

It will be noted that for values of $M_{\pi\Delta}$ or $M_{\pi n}$ near their respective thresholds, the calculated (output) value of $b$ is twice the

elastic-scattering value of 8.0 $(GeV/c)^{-2}$ used as input in Eq. (7). This substantial increase may be described as kinematical "feed-through" from the right to the left in the diagram of Fig. 3(a); any dependence on the variable $t_\Delta$ in Fig. 3(a) reflects itself kinematically as a dependence on the variable $t_p$. It is the steeply falling $(t_\Delta - m_\pi^2)^{-2}$ character of the $t_\Delta$ variation in either Eq. (7) or Eq. (18) which tends to force the $t_p$ dependence to be sharper than the input $\exp(8t_p)$ variation. The dependence in the matrix element on the sub-energy variables, however, subsequently modulates this effect and contributes to the variation of $b$ with $M_{\pi\Delta}$.

Such rapid variation of the slopes (on logarithmic plots) of momentum transfer distributions with the mass of produced states is a general feature of the double-peripheral approach to three particle production. Effects of this type have been observed experimentally notably in the missing-mass type of counter experiments[31] and also by several bubble-chamber groups.[32,33] Walker, in particular has described such a variation as an important aspect of the diffraction dissociation mechanism.[33,34] It is evident that one must be cautious in interpreting such systematic variation of the momentum transfer dependence with invariant mass; the above analysis shows that the effect is not obviously correlated with resonant behavior.

## B. Energy Dependence

Subject to the proviso that the $s_{p\pi}$ integration is carried out over its full range, the Regge-model matrix element, Eq.(7), yields a distribution in the $(\pi^-\Delta^{++})$ invariant mass whose peak position and

full width at half maximum are essentially independent of incident energy from 6.0 GeV/c to 100 GeV/c. The total cross section is likewise approximately energy independent. Similar statements apply to the calculation of $pp \to pn\pi^+$ reported earlier.[7]

C. Cuts in $s_{p\pi}$

The restriction in the previous section (IV) to the study of only those events for which $s_{p\pi} \geq 4.0\ (\text{GeV})^2$ is by no means fundamental. However, if one desires to represent data at smaller values of the $s_{p\pi}$ variable, then diagrams in addition to that given in Fig. 3(a) must be included in the computations; these would include (but are not limited to) diagrams of the same topology as that given in Fig. 3(a) but with P replaced by P' or $\rho$, for example. Evidently this argument does not imply the absence of a P contribution below $s_{p\pi} = 4.0\ (\text{GeV})^2$; rather it suggests, supported by Fig. 4(b), that other effects are more prominent there. By the same token, if one chooses to represent the data by using only the diagram shown in Fig. 3(a), whether in the Regge form or in the non-Reggeized OPE-DS[12] model, then either a cut in the $s_{p\pi}$ variable is in order or some other subtraction should be made to eliminate the non-Pomeranchuk effects. This last point is often ignored by researchers who use a non-Reggeized version of Fig. 3(a) for the purpose of calculating "background" contributions to processes such as $\pi p \to A_1 p$ or $Kp \to K^{**} p$.

D. Direct-Channel Diagrams

By way of emphasizing that the model discussed in this paper is one which seeks to interpret peripheral three-particle-final-state

processes entirely in terms of cross-channel exchange contributions, it should be noted that it is inappropriate to consider including a diagram of the direct channel variety, representing pole-term propagators in one of the subenergy variables (for examples, see Fig. 1(A) of the Ross-Yam analysis[12] or Fig. 6(b) of the Resnick paper[12]). For the $pp \rightarrow p\pi^-\Delta^{++}$ process studied in this paper, a direct-channel diagram, of the type to which reference is being made here, is one representing pp diffraction scattering with one of the final-state (off-mass-shell) protons subsequently dissociating into a $(\Delta^{++}\pi^-)$ pair. To include such a diagram along with that of Fig. 3(a) would likely result in the same type of double-counting that is involved in two-body processes if one adds direct-channel resonance terms to a so-called background formed of Regge-pole exchange contributions. This last remark is qualitatively evident if one regards the $\pi^-\Delta^{++}$ final state in Fig. 3(a) as resulting from the "quasi-two body" Pomeranchuk and proton $(p_2)$ interaction.

## VI. DISCUSSION

In several recent analyses, a double-Regge-pole-exchange-model approach of the type described here has provided good agreement with all experimental distributions even at near-threshold values of the invariant mass of a final pair of particles in a three-body final-state process. In addition to the proton-proton interaction studies already mentioned, in which data in the region of the 1400 MeV nucleon-isobar type enhancement has been fit, data from the reactions $\pi p \to \pi\rho p$ at 13.0 and 20.0 GeV/c[9] and coherent $\pi D \to \pi\rho D$ at 8.0 GeV/c[8] are also in agreement with calculations based on a Reggeized pion-Pomeranchuk double-peripheral diagram. These last two reactions give evidence for a broad $A_1$ (Mass $\approx$ 1100 MeV) enhancement in the $\pi\rho$ mass spectrum which the model adequately describes. Moreover, a partial wave analysis of the Regge-model amplitude predicts that 85% of the calculated $A_1$ enhancement is a $J^P = 1^+$ $(\pi\rho)$ system, in good agreement with the fraction determined experimentally in the 8.0 GeV/c study.[8]

It is inappropriate, however, to conclude from the results of these studies that either the $A_1$ or the N*(1400) effects observed in the above reactions are not resonances in the usual sense. For, whereas there has been no conclusive demonstration as yet that a cross-channel Regge-pole exchange description, on the one hand, and a direct-channel resonance interpretation are perfectly dual,[11] alternative modes of understanding, a growing body of information points in that direction. In quasi-two body scattering, the finite-energy-sum-rule[10] approach has

demonstrated that the appropriate sum over Regge-pole-exchange contributions in the cross channel provides an adequate semi-local average description of the imaginary part of the scattering amplitude, expressed in terms of direct channel resonance contributions. Moreover, partial wave analyses performed on the (asymptotically valid) Regge form of the amplitude and accepted even in the intermediate-energy resonance domain have demonstrated that resonance-like Argand-diagram circles are present in the Regge amplitude.[35]

Based on the fact that no poles in the direct channel energy-variable are present in the asymptotic Regge amplitude, objections have been raised to the interpretation of these circles as manifestations of resonances. Schmid countered these objections using an analogical reference to the Stirling approximation of the Gamma function;[35] however, a precise judgment on the duality issue awaits the development of a unique representation of the scattering amplitude, valid at all energies, and having Regge asymptotic behavior. Some progress in this regard is evident in a recent proposal by Veneziano.[36]

The relevance of this discussion to three particle-final-state problems is evident upon observing that insofar as the final state $\pi^-\Delta^{++}$, for example, is concerned, it can be regarded as being the end product in Fig. 3(a) of a quasi-two body proton-Pomeranchuk interaction, with pion exchange being the dominant cross-channel exchange mechanism. Thus, in effect, Reggeization has introduced a third, but possibly unifying, interpretation to the yet unsettled resonance versus kinematic enhancement question surrounding the experimental status of the $A_1$,

N*(1400), and $K\pi\pi$ - Q bump[37] effects. This controversy has the practical consequence of making it difficult to quote unambiguously values for "resonance" cross-sections in these mass regions.

The theoretical status of the calculations described here is somewhat primitive. Most fundamental, of course, is the matter of the use, at nonasymptotic values of $s_{\pi\Delta}$, of the unmodified Regge-form of the amplitude given in Eq. (7). Present justification relies on duality-type arguments[11] and on the not inconsiderable agreement with data on different reactions over a wide energy range. Further progress in this regard awaits the development, for example, of a Veneziano[36] type of representation for five-body processes which would have Regge asymptotic behavior in the two subenergy variables but provide a better near-threshold dependence on these variables.

Table I

Comparison of Regge and OPE model predictions with data for the location ($M_0$) of the peak and full width at half-maximum $\Gamma$ of the distribution in the invariant mass of the $(\pi^-\Delta^{++})$ system, for two values of the cutoff in the integration over the variable $t_\Delta$. The last line contrasts the predictions for the distribution in the Treiman-Yang angle. The OPE model contains a form-factor, as described in the text, with $\lambda = 1.0\ (\mathrm{GeV/c})^{-2}$.

| | OPE-DS ($\lambda = 1$) | Double-Regge ($\alpha'_\pi = 1.2$; $s_{0\pi} = 0.7$) | Exp. |
|---|---|---|---|
| $M_0$; $\lvert t_\Delta \rvert < 0.5$ | 1500 MeV | 1480 MeV | 1480 MeV |
| $M_0$; $\lvert t_\Delta \rvert < 1.0$ | 1580 MeV | 1520 MeV | 1500 MeV |
| $\Gamma$; $\lvert t_\Delta \rvert < 0.5$ | 420 MeV | 280 MeV | 200 MeV |
| $\Gamma$; $\lvert t_\Delta \rvert < 1.0$ | 540 MeV | 380 MeV | 320 MeV |
| Treiman-Yang; $\lvert t_\Delta \rvert < 0.8$ | Flat | 41% Asym. | See Fig. 6(a) |

Table II

Mass dependence of the differential cross section for $pp \to p\pi^-\Delta^{++}$ and $pp \to p\pi^+n$ at 28.5 GeV/c obtained from doubly-peripheral pion-Pomeranchuk mode; b is defined in Eq. (21) of the text.

| $pp \to p\pi^-\Delta^{++}$ | | $pp \to p\pi^+n$ | |
|---|---|---|---|
| Mass ($\pi\Delta$) (GeV) | b $(GeV/c)^{-2}$ | Mass ($\pi n$) (GeV) | b $(GeV/c)^{-2}$ |
| 1.40 | 14.0 | 1.10 | 18.0 |
| 1.50 | 11.5 | 1.20 | 12.5 |
| 1.60 | 10.0 | 1.30 | 9.5 |
| 1.80 | 8.0 | 1.50 | 7.0 |
| 2.00 | 5.2 | 1.80 | 4.5 |

ACKNOWLEDGMENTS

It is a pleasure to thank Professor Geoffrey F. Chew and Dr. Robert Panvini for several valuable discussions and for critical comments on this manuscript. A major portion of this study was undertaken while I was a guest of the Bubble Chamber Group at Brookhaven National Laboratory during the summer of 1968; I am grateful to Dr. Ralph Shutt and other members of the Group for their hospitality and provocative discussions. The assistance of Dr. Panvini and Mr. Edwin Ellis in understanding the experimental distributions was invaluable. I am indebted to Dartmouth College for a leave of absence and Faculty Fellowship support.

## FOOTNOTES AND REFERENCES

* This work was supported in part by the U.S. Atomic Energy Commission.

+ On leave from Dartmouth College, Hanover, New Hampshire.

++ Present address.

1. N. F. Bali, G. F. Chew, and A. Pignotti, Phys. Rev. Letters 19, 614 (1967) and Phys. Rev. 163, 1572 (1967). An extensive list of references to earlier work may be found in G. F. Chew and A. Pignotti, UCRL-18275, June, 1968, to be published in Phys. Rev.

2. H. M. Chan, K. Kajantie, and G. Ranft, Nuovo Cimento 49, 157 (1967); H. M. Chan et al., Nuovo Cimento 51, 696 (1967). For a partial review of the double-Regge-pole model approach, including references to phenomenological fits, see articles by Chan Hong-Mo and S. Ratti in Topical Conference on High-Energy Collisions of Hadrons, CERN, January, 1968.

3. F. Zachariasen and G. Zweig, Phys. Rev. 160, 1322 and 1326 (1967).

4. R. G. Roberts and G. M. Fraser, Phys. Rev. 159, 1297 (1967).

5. E. L. Berger, Phys. Rev. 166, 1525 (1968).

6. E. L. Berger et al., Phys. Rev. Letters 20, 964 (1968).

7. E. L. Berger, Phys. Rev. Letters 21, 701 (1968).

8. A. M. Cnops et al., preprint, Brookhaven National Laboratory 12677, July, 1968 and Ian O. Skillicorn, private communication.

9. M. L. Ioffredo et al., Phys. Rev. Letters 21, 1212 (1968).

10. R. Dolen, D. Horn, and C. Schmid, Phys. Rev. 166, 1768 (1968); K. Igi and S. Matsuda, Phys. Rev. Letters 18, 625 (1967).

11. G. F. Chew and A. Pignotti, Phys. Rev. Letters 20, 1078 (1968); G. F. Chew, Comments on Nuclear and Particle Physics 2, 74 (1968).

12. L. Stodolsky, Phys. Rev. Letters 18, 973 (1967); M. Ross and Y. Yam, ibid 19, 546 (1967); U. Maor, Ann. Phys. (N.Y.) 41, 456 (1967). L. Resnick, Phys. Rev. 150, 1292 (1966). References to previous work may be found in these papers.

13. The data were derived from a Brookhaven National Laboratory Bubble Chamber group study of pp interactions as reported in P. L. Connolly et al., Brookhaven National Laboratory 11980; W. E. Ellis et al., Brookhaven National Laboratory 12673, submitted to the 14th International Conference on High Energy Physics, Vienna, 1968; and W. E. Ellis et al., Phys. Rev. Letters 21, 697 (1968).

14. The metric use here is specified by $q \cdot q = q_0^2 - \vec{q} \cdot \vec{q} = m^2$, where $q$ is a four-vector.

15. At fixed $s$, the invariant amplitude for reaction (1) is a function of four independent variables which are taken here to be the set of Lorentz-invariant quantities defined in Fig. 1: two subenergy variables, $s_1$ and $s_2$, and two momentum transfer variables, $t_1$ and $t_2$.

16. About 500 events appear necessary for an adequate study of three-body-final-state production models at fixed $s$.

17. An example of this type has been studied by G. Alexander et al., UCRL-18321, July, 1968; submitted to Phys. Rev.

18. W. Rarita et al., Phys. Rev. 165, 1615 (1968).

19. At high-energy, the slope on a logarithmic plot of the $\pi p$ elastic $d\sigma/dt_p$ is approximately the value 8.0 $(GeV/c)^{-2}$ used here; see K. J. Foley et al., Phys. Rev. Letters 11, 425 (1963); D. Harting et al., Nuovo Cimento 38, 60 (1965); and Ref. 18.

20. In employing $(s_{\pi\Delta}\cdots)^{\alpha_\pi}$ and $(s_{P\pi}\cdots)^{\alpha_P}$, the form given by the numerator of the cosh $\xi_i$ variables of the Toller analysis (Ref. 1) is retained. See Eqs. (8) and (9). Especially since the continuation is made here to near threshold values of $s_{\pi\Delta}$, it is not clear that this choice is preferable to simply using $(s_{\pi\Delta})^{\alpha_\pi}$.

21. Actually, most researchers studying quasi two body interactions concern themselves only with small values of $t$ and extract factors such as $(\alpha + 1)(\alpha + 2)$ from the $[\Gamma(1 + \alpha)]^{-1}$. For examples, see Ref. 18, and F. Arbab and C. B. Chiu, Phys. Rev. 147, 1047 (1966).

22. This may be derived by writing the invariant amplitude for the $p\pi\Delta$ coupling, in Fig. 3(a), as

$$M = G\,\bar{u}_\nu(q_2)\,[p_2 - q_2]_\nu\,u(p_2) \quad ,$$

where $u_\nu(q_2)$ is a 16 component Lorentz-vector Dirac spinor and then evaluating $G$ in terms of the width of the $\Delta$. See, for example, J. D. Jackson and H. Pilkuhn, Nuovo Cimento 33, 906 (1964).

23. Consult, for example, G. Kallen, Elementary Particle Physics (Addison-Wesley, Inc., Reading, Massachusetts, 1964), p. 18.

24. If $\sigma_{TOT}$ in Eq. (16) is expressed in mb, and all other units are in GeV, in order for Eqs. (6) and (7) to yield a cross-section in mb, an additional conversion factor of 2.5 $mb^{-1}$ $(GeV)^{-2}$ must be supplied on the right-hand side of Eq. (16).

25. The mass of the $\sigma$ would have to be 450 MeV or less, however.

26. I am indebted to W. Edwin Ellis for assistance with the maximum likelihood fit.

27. In obtaining the normalization, the values $\Gamma = 120$ MeV and $\sigma_{TOT,\pi p} = 28$ mb were used in Eq. (12) and (16). See also Footnote 24. The data correspond to a cross section of 0.87 μb/event.

28. Additional dependence on $t_\Delta$, associated with the spin structure of the $\Delta^{++}$, was evaluated at $t_\Delta = m_\pi^2$ and absorbed into $N_0$.

29. The definition of $\varphi$ used in Ref. 6 differs slightly from that in this work; they are related by $\varphi(6.6) = \varphi(28.5) + \pi$.

30. G. Fox, private communication.

31. E. W. Anderson et al., Phys. Rev. Letters 16, 855 (1966); G. Belletini et al., Physics Letters 18, 167 (1965); J. M. Blair et al., Phys. Rev. Letters 17, 789 (1966); K. J. Foley et al., ibid. 19, 397 (1967).

32. J. Bartsch et al., Physics Letters 27B, 336 (1968).

33. W. D. Walker et al., Phys. Rev. Letters 20, 133 (1968); A. F. Garfinkel et al., Wisconsin preprint, August, 1968.

34. M. L. Good and W. D. Walker, Phys. Rev. 120, 1857 (1960).

35. C. Schmid, Phys. Rev. Letters 20, 689 (1968); P. D. B. Collins, R. C. Johnson, and E. Squires, Physics Letters 27B, 23 (1968);

C. B. Chiu and A. Kotanski, CERN preprints Ref. Th. 907 and 939, (1968); V. Alessandrini et al., CERN preprint Th. 922 (1968).

36. G. Veneziano, Nuovo Cimento 57A, 189 (1968).

37. G. Goldhaber et al., Phys. Rev. Letters 19, 972 (1967) and references therein.

FIGURE CAPTIONS

Fig. 1. General double-Regge-pole-exchange diagram for the process $m_1 + m_2 \to \mu_1 + \mu + \mu_2$. The $p_i$ and $q_i$ are four-momenta and the $m_i$ and $\mu_i$ are masses. $s_1 = (q_1 + q)^2$, $s_2 = (q_2 + q)^2$, $t_2 = (q_2 - p_2)^2$, $t_1 = (q_1 - p_1)^2$, $s = (p_1 + p_2)^2$. The $\alpha_j$ denote Regge trajectories.

Fig. 2. Diagrams containing Pomeranchuk (P) exchange which contribute to $pp \to p\pi^-\Delta^{++}$; M denotes a meson-type and B a baryon-type trajectory.

Fig. 3. (a) Dominant double-Regge-pole exchange diagram for the reaction $pp \to p\pi\Delta^{++}$; $\alpha_P$ denotes the Pomeranchuk and $\alpha_\pi$ the pion-trajectory. The $p_i$ and $q_i$ are four-momenta. $s_{p\pi} = (q_1 + q)^2$, $s_{\pi\Delta} = (q_2 + q)^2$, $t_\Delta = (q_2 - p_2)^2$, $t_p = (q_1 - p_1)^2$, $s = (p_1 + p_2)^2$.

(b) Triple-exchange four-particle final state diagram representing background contribution.

Fig. 4. (a) Distribution in the invariant four-momentum transfer-squared to the $\Delta^{++}$ for the reaction $pp \to p\pi^-\Delta^{++}$ at 28.5 GeV/c. In the plot, there are 445 events for which $s_{p\pi^-} > 4.0\ (\text{GeV})^2$. The solid curve is the Regge model fit with $\alpha'_\pi = 1.2\ (\text{GeV})^{-2}$ and $s_{0\pi} = 0.7\ (\text{GeV})^2$.

(b) Distribution in the invariant four-momentum-transfer squared to the final p for the process $pp \to p\pi^-\Delta^{++}$, for events in the region $s_{p\pi^-} > 4.0\ (\text{GeV})^2$ and

$|t_\Delta| < 0.8$ (GeV/c)$^2$. In the first bin, the dashed line corresponds to twice the numer of those events associated with backwards $\Delta^{++}\pi^-$ production only.

Fig. 5. (a) Distribution in the invariant-mass-squared of the $(\Delta^{++}\pi^-)$ system containing events for which $s_{P\pi^-} > 4.0$ (GeV)$^2$ and $|t_\Delta| < 1.0$ (GeV/c)$^2$.

(b) Distribution in the invariant-mass-squared of the $(p\pi^-)$ for events with $|t_\Delta| < 0.8$ (GeV/c)$^2$. The histogram is not plotted below $s_{p\pi} = 3.0$ (GeV)$^2$ which is outside the range of validity of the present calculation.

Fig. 6. (a) Distribution in the Treiman-Yang angle for $p\pi^-\Delta^{++}$ defined in the $p\pi^-$ rest frame as

$$\phi = \cos^{-1}\left[(\hat{p_1 \times q_1}) \cdot (\hat{p_2 \times q_2})\right]$$

where the $p_i$ and $q_i$ in this expression are three-vectors specified by reference to Fig. 3 (a).

(b) Distribution in the Toller angle,

$$\omega = \cos^{-1}\left[(\hat{p_1 \times q_1}) \cdot (\hat{p_2 \times q_2})\right],$$

measured in the rest frame of the $\pi^-$. The Regge model fits the distribution without requiring explicit $\omega$ dependence in the matrix element. Both (a) and (b) contain 349 events for which $s_{p\pi} > 4.0$ (GeV)$^2$ and $|t_\Delta| < 0.8$ (GeV/c)$^2$.

Fig. 7. Distribution in the cosine of the $\Delta^{++}$ production angle. With reference to Fig. 3 (a), the angle is defined by $\cos\theta_\Delta = \vec{q}_2 \cdot \vec{p}_2 / |\vec{q}_2||\vec{p}_2|$ where the three-vectors $\vec{q}_2$ and

$\vec{p}_2$ are measured in the frame of reference in which the $(\pi^-\Delta^{++})$ system is at rest. The selections imposed here were $|t_p| \leqslant 0.3$ $(\mathrm{GeV/c})^2$, Mass $(\pi\Delta) \leqslant 1.6$ GeV and $s_{p\pi} \geqslant 4.0$ $(\mathrm{GeV})^2$. The solid line is the Regge model prediction; the dashed curve is the model prediction with the selection on $s_{p\pi}$ removed.

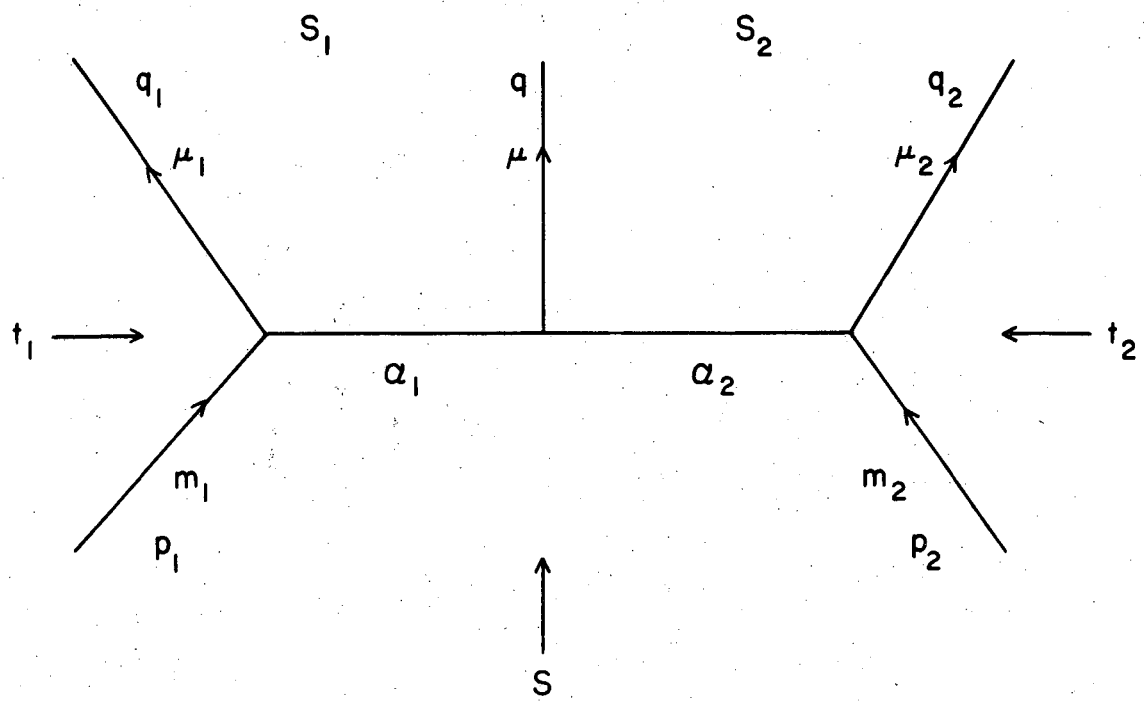


XBL 6810-6051

Fig. 1

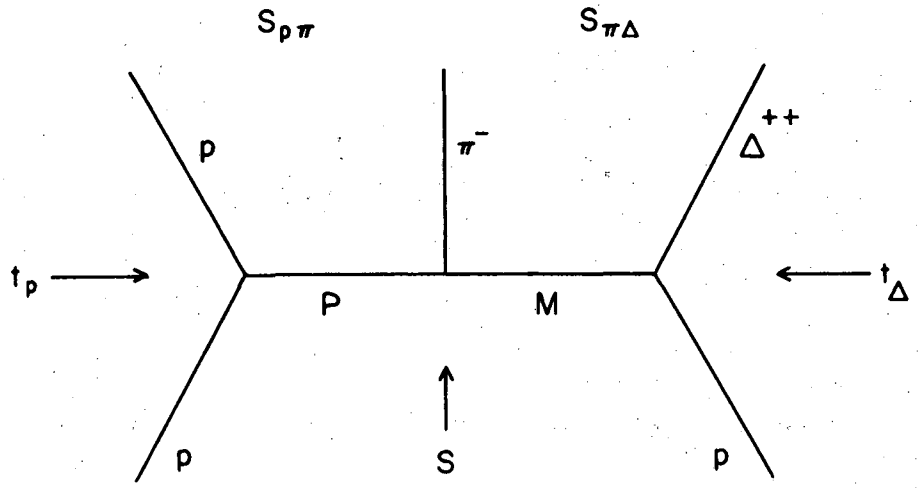


(a)

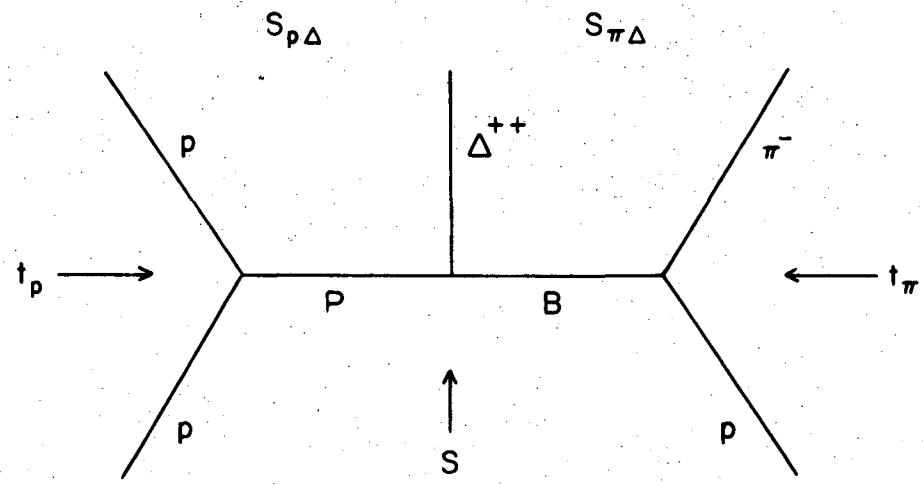


(b)

XBL 6810-6052

Fig. 2

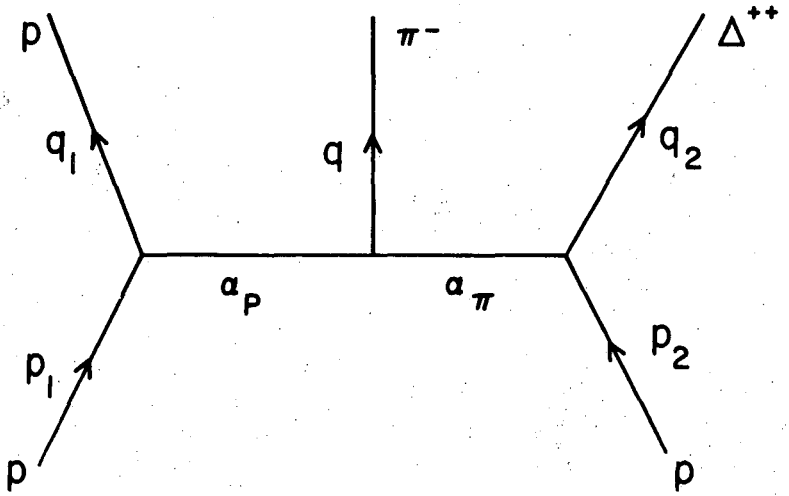


(a)

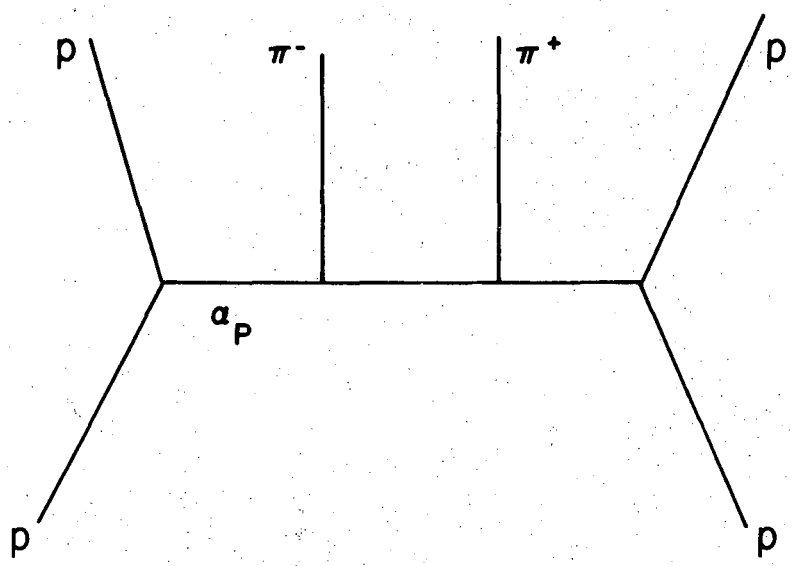


(b)

XBL 6810-6053

Fig. 3

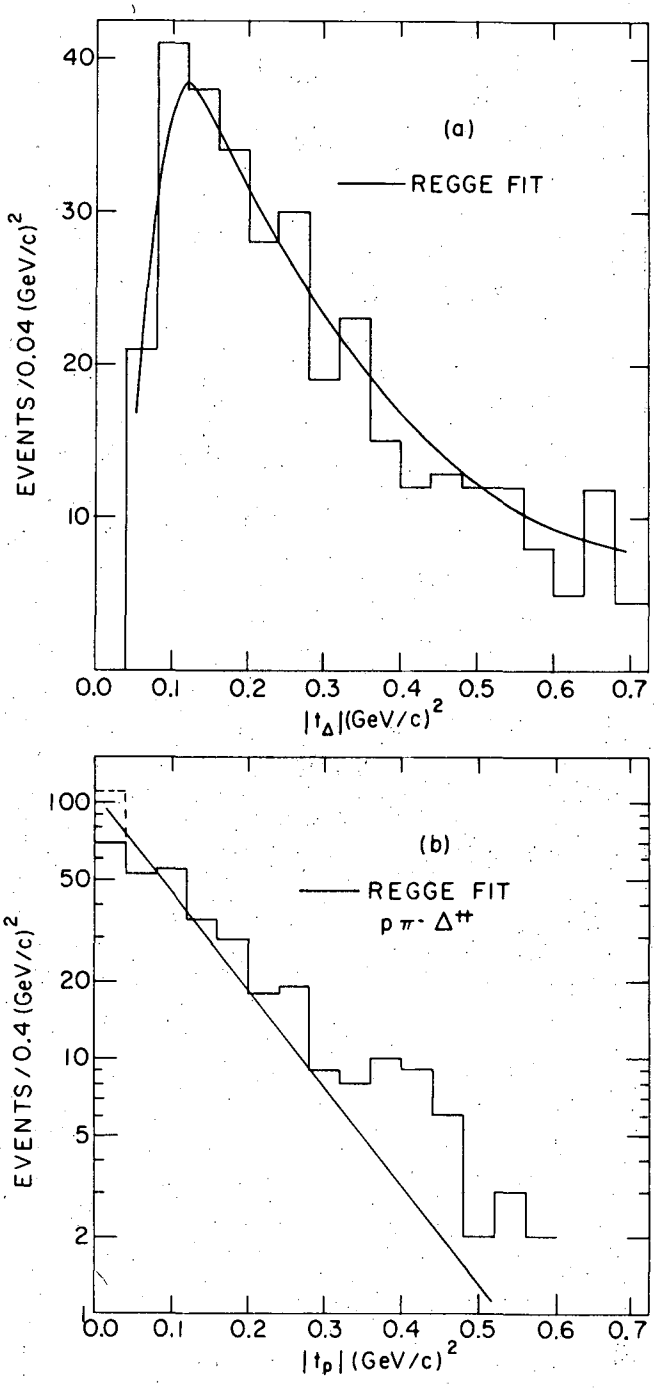


XBL 6810-6054

Fig. 4

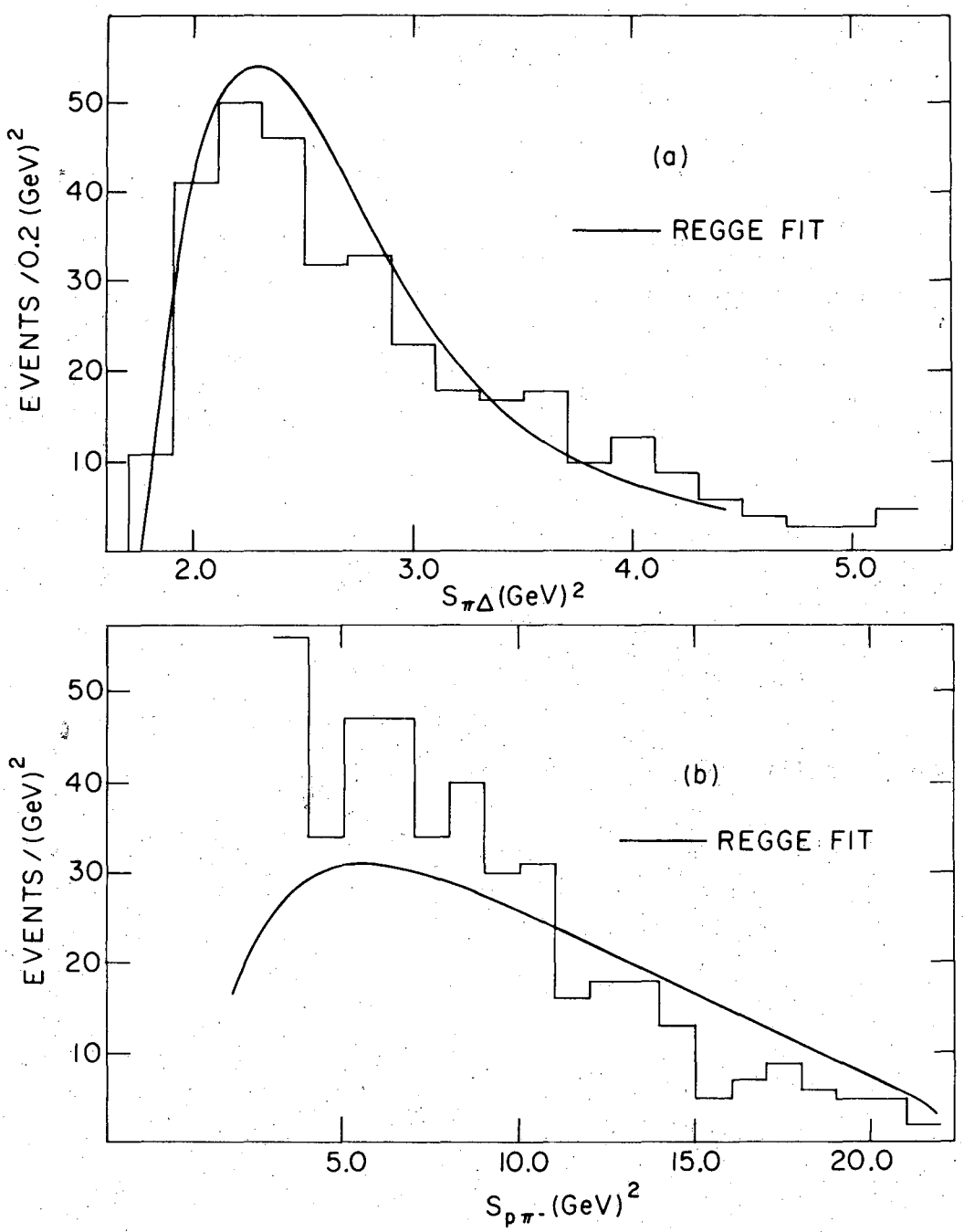


XBL 6810-6055

Fig. 5

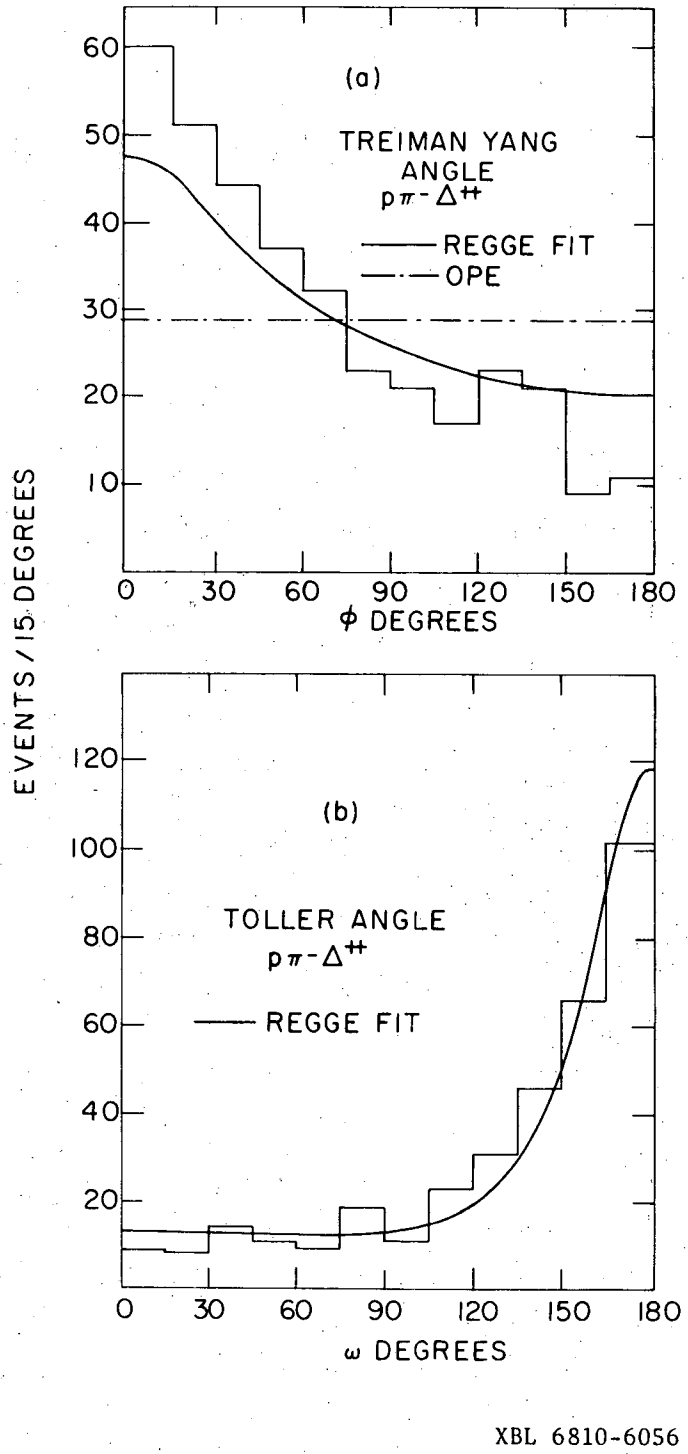
(a)
TREIMAN YANG ANGLE
pπ-Δ++
REGGE FIT
OPE
EVENTS / 15 DEGREES
φ DEGREES
(b)
TOLLER ANGLE
pπ-Δ++
REGGE FIT
ω DEGREES
XBL 6810-6056

Fig. 6

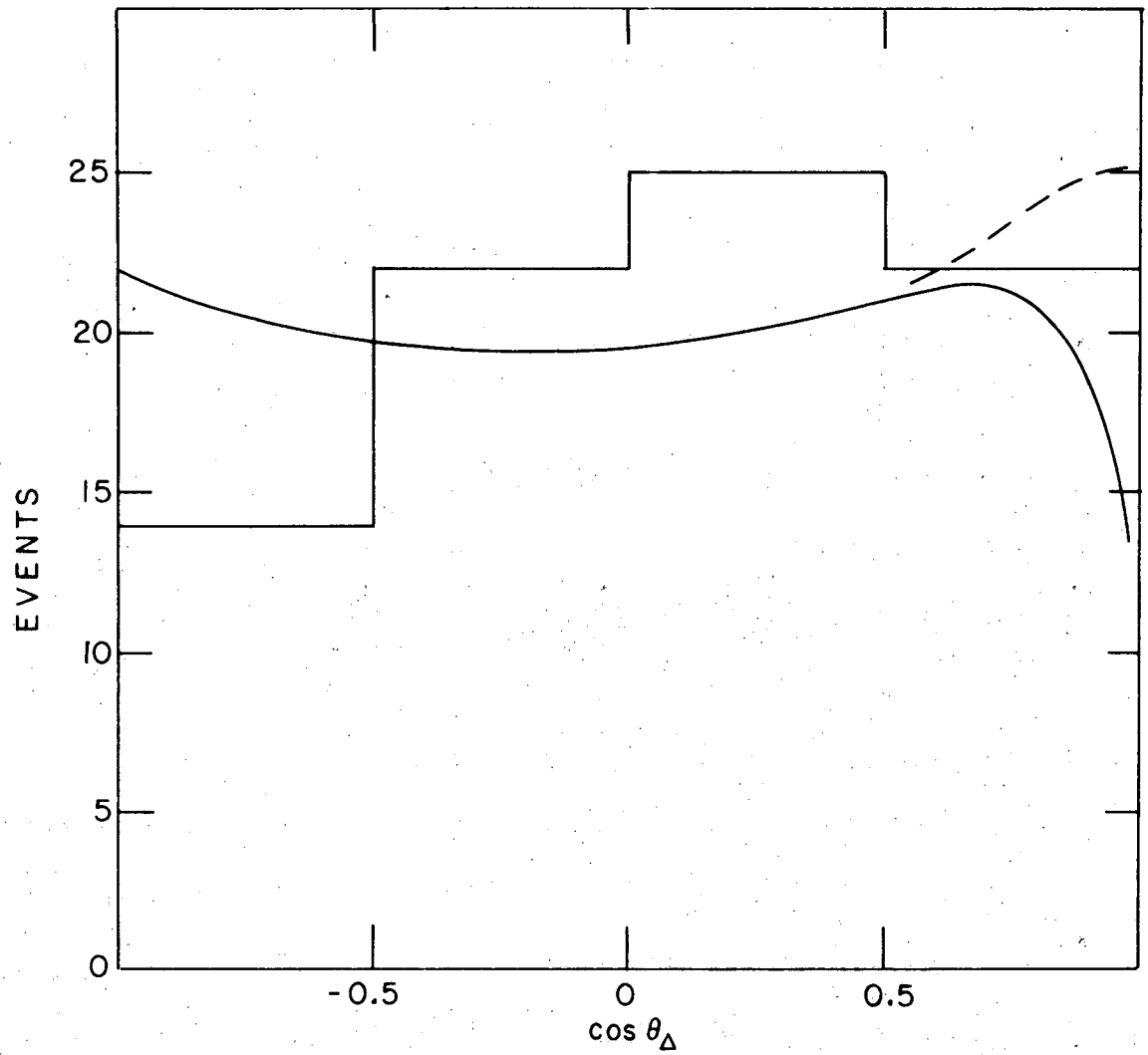


XBL 6810-6057

Fig. 7